ELECTROTHERMAL STRESS-STRAIN IN ANCILLARY PARTS OF AN ALUMINUM ELECTROLYSIS CELL

MARIN PETRE[1], ALEXANDRU MIHAIL MOREGA[2,3], MARIAN CILIANU[4]

Key words: Aluminum electrolysis, Electro-thermal stress, Heat transfer, Numerical modeling, Finite element.

In the last years ALRO Slatina plant was subject to the modernization of the technological process of aluminum production by changes in the electrolysis cell, which led to superior economic and technological performance. The increase in the electrical power per cell is accompanied by the increase in the size (and weight) of the cathode and anode blocks that, in turn, may enhance the strain of the supporting anodic frame and, implicitly, the strain of the connections between it and the omnibus bars. To better understand these effects and to highlight the possible risk areas, we investigate – by mathematical modeling and numerical (finite element) simulation – the thermally induced mechanical stress for the anodic frame and the flexible beam.

1. **INTRODUCTION**

Primary aluminum is obtained in electrolysis cells through a series of complex interactions between various physical and chemical phenomena: electro-chemical reactions, mass and heat transfer, electromagnetism, fluid dynamics, and structural mechanics [1–5]. One of the central concerns with ever increasing cells (in terms of power) is the thermal induced stress that leads to deformations of the cell structural parts (case, anodic frame, collector bars, *etc*.) – a menace to the life duration of the cell. Due to the anode block volume growing and, implicitly, of its weight (1,200 kg, the weight of the assembly anode) with the electrical power of the cell, a certain deformation of the anodic frame is observed. Therefore the knowledge of their order of magnitude is needed to find means and solutions to compensate for the thermal induced deformations.

[1] S.C. ALRO S.A. Slatina, Olt, Romania; E-mail: marin.petre@yahoo.com
[2] Faculty of Electrical Engineering, "Politehnica" University of Bucharest, Splaiul Independenței no. 313, sector 6, Bucharest, 060042, Romania; E-mail: amm@iem.pub.ro
[3] "Gh. Mihoc – C. Iacob" Institute of Statistical Mathematics and Applied Mathematics, Romanian Academy, Calea 13 Septembrie no.13, 050711, Bucharest; Romania, E-mail: amm@iem.pub.ro
[4] S.C. ALRO S.A. Slatina, Olt, Romania; E-mail: mcilianu@alro.ro

Rev. Roum. Sci. Techn. – Électrotechn. et Énerg., **57**, *1*, p. 30–39, Bucarest, 2012

The mechanical structure of an electrolysis plant is complex. Typically, the electrolysis cells are electrically connected, in-between, in series by electric conductors (called either *busbars* or *omnibus bars*) made of aluminum plates, whose cross sections are sized to match the electrical current density. The electrical connection of the anodic assembly of the electrolysis cell to the omnibus bars, which feeds the cell with electrical power, consists of a number of fascicular connections, each made of aluminum sheets 2–3 mm thick, with the end-parts welded in groups of 10–20 pieces/beam. The number of fascicles of a flexible beam depends on the working electrical current that is conveys. The flexible connections are electrically welded with an end to the respective omnibus bar, and the opposite end to the aluminum anodic frame of the electrolysis cell, thus achieving the entry connection of the continuous electrical current in the cell [2]. Inside the cell, the electrical current flows through the anodes, bath, molten metal, the cathode blocks, to be finally drained through the end parts of the collector steel bars that are embedded in the cathode blocks. The current is conveyed out of the cell through flexible connections provided between each end of the cathode bar assembled in the cathode block and the omnibus.

From another perspective, numerical simulation has reached the level where it becomes one of the tools used in investigating complex problems such as the electro-thermal fields and induced stresses in structures of a CAD level of detail [4], [6−8]. In this paper we investigate by numerical simulation the thermally induced stress-strain by the anodic frame and the flexible beam. The model we developed combines the stress-strain analysis with the DC (electrokinetic) current flow and with the associated heat transfer by conduction, that is, a multiphysics couplings between Joule heating, heat transfer within the anodic frame and the flexible beam, and its thermal expansion.

The results obtained are useful in assessing the thermal stress and optimizing the design of the anodic frame and the flexible beam. The electrical current and the thermal field were calculated by using a fully 3-D electrokinetic model of aluminum electrolysis cell and are reported in [9–11]. The anode height is that of a mid-life anode, *i.e*. 0.41m. Here, we focus on the structural analysis induced by the electro-thermal stresses that occur in the anodic frame and the flexible beam.

2. **THE ANODIC FRAME**

The aluminum electrolysis cell in ALRO Slatina plant is equipped with 16 pre-baked carbon blocks. Hot carbonic paste (petroleum coke and coal tar pitch) is

the base material for these blocks. Pre-baked anode blocks are used in the electrolysis cells as assemblies that convey the current, mounted on an aluminum anodic rods, continued with bimetal aluminum-steel connectors and a steel structures, fixed to the existing holes in the anode blocks by iron casting.

The aluminum-steel connectors are obtained by explosive welding. The steel structure, which unites the anode rod with the anode carbon blocks, may have different forms, depending on the anodes type used in the process (either bipod, tripod or tetrapod). The steel structure for the anode of the electrolysis cell at the ALRO plant has the form of tetrapod [3]. The rod sustaining the assembled anode is fastened to the mobile frame of the electrolysis cell, and may be removed and replaced after the anode consumption in the electrolysis process. Fig. 1 presents the CAD [14] concept that embodies this structure.

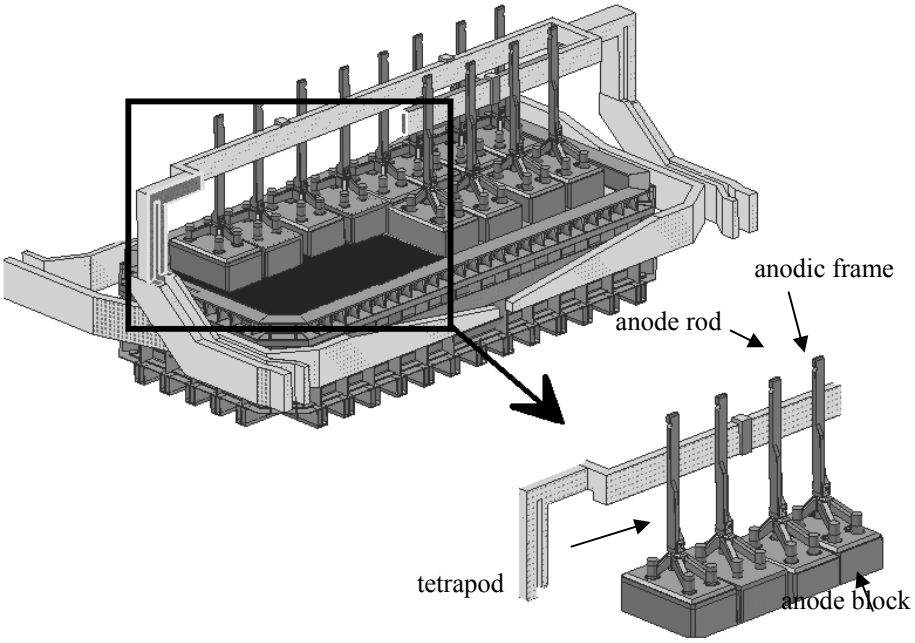

Fig. 1 – Electrolysis cell and the studied model – the anodic frame made of four anode blocks.

To reduce the computational complexity, the cell design was cropped using symmetry. This approach turns out to be especially important in containing the magnetic field problem, not reported here, which requires a comprehensive computational domain [12]. Next, we present the mathematical model and

numerical simulation results for the structural analysis induced by the electro-thermal stresses that occur in the anodic frame and the flexible beam.

3. **THE MATHEMATICAL MODEL**

The steady state boundary value problem of the thermally produced stress in the anodic frame and the flexible beam is made of: (1) the electrokinetic (DC) current in the flexible beam, anodic frame and anode block; (2) the associated heat transfer problem; (3) the thermally induced stress-strain in this structure.

To reduce the complexity of the problem and to contain the numerical simulations within the available hardware and software resources limits while sticking to an as realistic as possible description of the phenomena and cell, we considered to following strategy. First, the DC problem is solved for the entire cell. Next, the resistive (Joule) power thus obtained is utilized as source for the heat transfer problem within the cell. These two steps, reported elsewhere [10-12], concern the entire cell. Finally, the structural problem is solved for a reduced model: the anodic frame and the flexible beam. We assume that aluminum flexible connections form a whole block of aluminum, due to its negligible small size (2-3 mm thick) as compared to the size of the entire model.

3.1. THE ELECTRICAL FIELD PROBLEM

The electrical field problem is described by [12]

$$-\nabla\cdot(\sigma\nabla V)=0, \tag{1}$$

where V is the electrokinetic potential, and σ is the electrical conductivity.

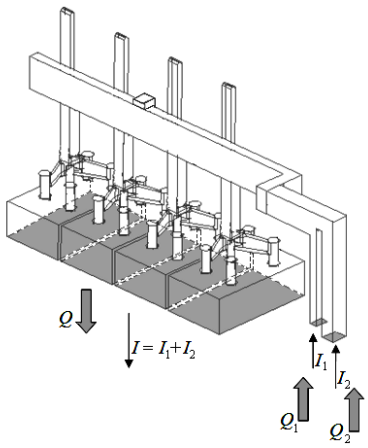

Fig. 2 – Electrical and heat currents. Heat transfer by free convection to the ambient is not shown.

The boundary conditions (BCs) that close the electrical field model are

- *for the flexible beam current inlet ports*

$$-\mathbf{n}\cdot\mathbf{J} = J_n; \tag{2}$$

- *for the anode base outlet ports* (*ends*)

$$V = 0; \tag{3}$$

- *for all other parts of the boundary* (*electrical insulation*)

$$\mathbf{n}\cdot\mathbf{J} = 0. \tag{4}$$

Here **n** is the unit vector normal to the surface and J_n is the normal component of the electrical current density.

3.2. THE HEAT TRANSFER PROBLEM

The heat transfer problem is described by the partial differential equation

$$\nabla\cdot\left(-k\nabla T\right) = P_J, \tag{6}$$

where T is temperature, k is the thermal conductivity and P_J is the internal heat source – the resistive (Joule) heating power [9–11]. The boundary conditions model the heat flux released by the anode base and the heat released through the flexible beam

$$-\mathbf{n}\cdot\left(-k\nabla T\right) = q_n. \tag{7}$$

They are the outcome of the electrokinetic and heat transfer problems [10–12]. Elsewhere we assume (natural) convection heat transfer conditions, *i.e.*

$$-\mathbf{n}\cdot\left(-k\nabla T\right) = h\left(T_{inf} - T\right), \tag{8}$$

where h is the convection heat transfer coefficient (here, h = 15 W/m^{2}K), T_{inf} is the external temperature, and q_n is the outward normal heat flux.

The anodic frame, flexible beam and the anode rod are made of aluminum, while the tetrapod is made of steel and anode block is made of graphite. In this study, all materials are assumed isotropic and linear, with constant thermal and electrical properties set at appropriate working temperatures. In the structural stress-strain analysis part the materials are assumed isotropic.

The BCs for the structural model are of "free" (unconstrained) type, except for the symmetry boundaries that are not to deform along the directions perpendicular to the symmetry planes, respectively (Fig. 3). Specifically for the flexible beam cross section and the anodic frame clamping area (light grey)

$$R_x = 0,\ R_y = 0,\ R_z = 0\,, \tag{9}$$

and for the symmetry planes (dark grey) – longitudinal for the anodic frame, and transversal for the flexible beam – the BCs are of "free" type in the plane and "fixed" in the out-of-plane direction, *i.e*

$$R_n = 0. \tag{10}$$

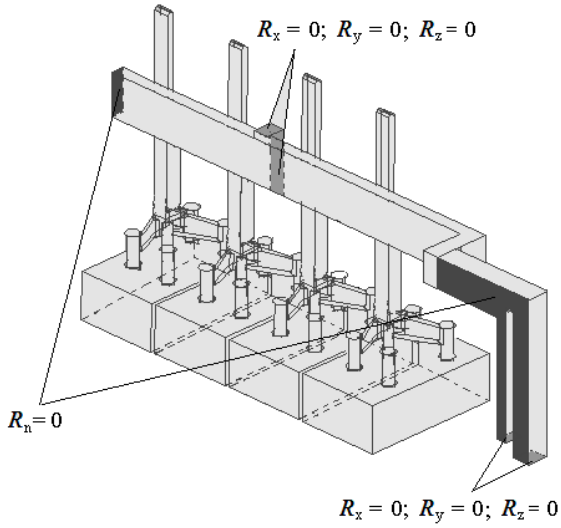

Fig. 3 – Constraints (BCs) for the stress-strain model: *fixed* type (light grey); *symmetry planes* (dark grey); the rest is set *free*.

The stress-strain constitutive law is defined based on a strain energy density function

$$W = W(I_1, I_2, I_3), \tag{11}$$

where $I_1 = \text{trace}(C)$, $I_2 = \left[I_1^2 - \text{trace}(C^2)\right]$, $I_3 = \det(C) = J^2$, and $C = \mathbf{F}^T\mathbf{F}$ is the right Cauchy-Green tensor [15–16], **F** is the deformation gradient, *J* is the ratio between the current and the original volume. For thermal expansion, a stress-free volume change occurs, and *J* is replaced by the elastic part of the total volume change

$$J_{elastic} = J/J_{th} = J/(1+\varepsilon_{th})^3, \tag{12}$$

where $\varepsilon_{th} = \alpha(T - T_{ref})$ is the thermal strain, α is the thermal expansion coefficient, T_{ref} is the reference temperature (taken T_{inf}, here). The stresses, *S*, are computed by deriving *W* with respect to Green-strains, *E*, *i.e*. $S = \partial W/\partial E$. The mathematical model (1)–(12) was solved numerically by the Galerkin FEM [15]. A similar problem and its solution may be found in [10–12].

4. NUMERICAL SIMULATION RESULTS. DISCUSSION

The electrical current and heat flows obtained by numerical simulation for the entire cell are then used to obtain the heat and electrical currents in a reduced model (Fig. 2). Experimental measurement concerning the voltage drop on the anodic frame, flexible beam and for each anode assembly were performed to assess the accuracy of the numerical results. All these measurements were conducted on a group of 15 cells, and they compare satisfactorily well to the numerical simulation results [3, 4]. As expected, the highest temperatures occur at the base of the anode block because this is in direct contact with the electrolyte layer.

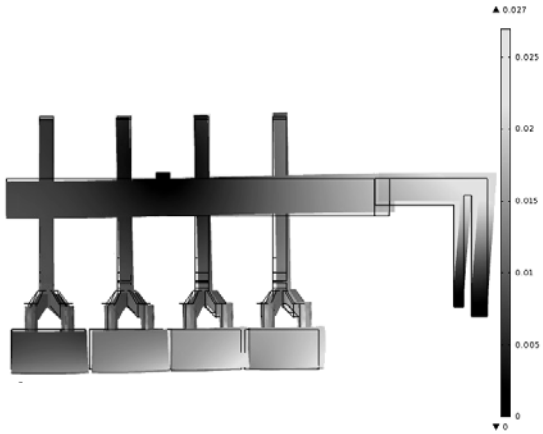

Fig. 4 – Displacement (amplified 3.5 times for better view) – side view.

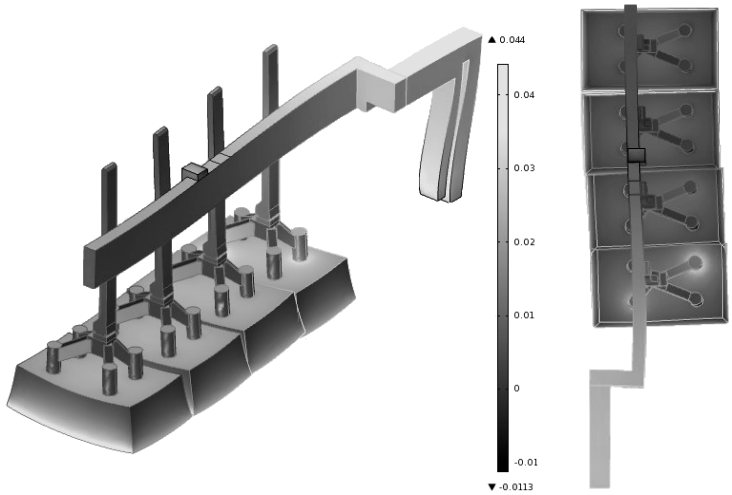

Fig. 5 – Thermally induced displacements (amplified 10 times for better view).

Figs. 4 and 5 display the deformations of the aluminum flexible sheets and anodic blocks that lead to the displacements of the anodic frame.

Table 1 lists the average, translational displacements of the particular surfaces, obtained by numerical simulations.

Table 1

Average translational displacements obtained by numerical simulation – under weight and under weight plus thermal stress

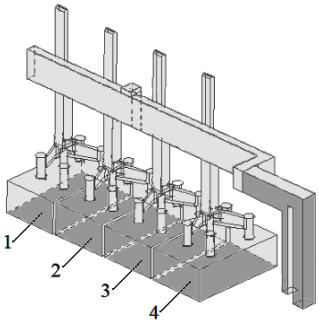

Surface	Due to weight [mm]	Due to weight and heat [mm]	Relative values [%]
1	6.698	6.393	4.55
2	6.617	6.363	3.84
3	6.109	5.999	1.80
4	6.466	6.624	2.44

The *average* displacements are of the order of millimetre. However, considering that the spacing between the anodes' surfaces and the molten bath is about 5 cm these displacements are important.

a. Anode assembly.

b. Anode assembly – thermo vision image.

Fig. 6 – Thermovision image of the model (for one anode assembly).

Another interesting observation is that under combined weight and thermal stress the average displacements of faces 1 through 3 are smaller than those under

weight only, and conversely for face 4. This effect may be explained by the structural complexity of the anodic frame.

To check the thermal load of the anode assembly, flexible beam and anodic frame in the real cell we used thermal vision measurements (Fig. 6) [17]. The recorded temperatures are in good agreement with the numerical simulations [12], which suggests that the thermally induced stress-strain in the structure was evaluated in realistic conditions.

Further more, experimental measurements on the voltage drops on the anodic frame, flexible beam, and for each anode assembly were also performed for a group of 15 cells that compare satisfactorily well to the numerical simulation results [10–12].

5. **CONCLUSIONS**

In this paper we report a mathematical model and numerical simulation results for the thermo-structural analysis of the anodic frame, aluminum flexible connections, and anode assembly induced by electro-thermal stresses. We used as input the results (heat flow, inward current flow) obtained for the electrokinetic and heat transfer model of the whole electrolysis cell [10–12].

The numerical simulations results obtained for temperature and voltage are in good agreement with experimental data available for the cell under investigation.

The thermally induced mechanical stresses are in accordance with the observations in the electrolysis pot-rooms. Although only in the range of millimeters these displacements are important considering that the spacing between the anodes bottom surfaces and the bath is only about 5 cm. This is an important part for the experimental validation, the object of future research.

The findings are useful to better understand the mechanical response to heat induced deformations, and to provide for design solutions aimed at preventing the changes made and to highlight the areas with a possible risk in the aluminum electrolysis cell.

Received on 22 September 2011

REFERENCES

1. Cr. Stănescu, C. Rădulescu, G. Dobra, M. Atanasiu, S. Manaktala, *Cell capacity increase program at ALRO*, in: *Light Metals*, Ed. H. Kvande, TMS (The Minerals, Metals & Materials Society), 2005.
2. I. Fara, N. Panait, G. Dobra, M. Cilianu, s.a., *Aluminiul de la materie primă la produs finit*, Edit. Tehnică, Bucureşti, 2000.

3. Gh. Dobra, C. Rădulescu, S. Manaktala, Cr. Stănescu, *Cell for obtaining electrolytic aluminum, at the intensity of 120 kA*, Patent 09.08.2004.
4. J.N. Bruggeman, *Pot heat balance fundamentals*, Eds. B.J. James, M. Skyllas-Kazacos and B.J. Welch, Proc. of the 6th Australian Aluminum Smelting Workshop, 1998, pp. 167-189.
5. I.F. Hănțilă, M. Vasiliu, A. Moraru, M. Maricaru, *Utilizing the polarization method for solving a nonlinear magnetic shielding problem*, Rev. Roum. Sci. Techn. – Électrotechn. et Énerg., **55**, *2*, pp. 123–131, 2010.
6. M. Dupuis, *Mathematical modeling of aluminum reduction cell potshell deformation*, in: *Light Metals*, TMS (The Minerals, Metals & Materials Society), 2010.
7. D. Molenaar, K. Ding, A. Kapoor, *Development of industrial benchmark finite element analysis model to study energy efficient electrical connections for primary aluminum smelters*, in: *Light Metals*, Ed. S.J. Lindsay, TMS (The Minerals, Metals & Materials Society), 2011, pp. 985-990.
8. S. Beier, J.J.J. Chen, H. Fortin, M. Fafard, *FEM analysis of the anode connection in aluminum reduction cells*, in *Light Metals*, Ed. S.J. Lindsay, TMS (The Minerals, Metals & Materials Society), 2011, pp. 978-984.
9. M. Dupuis, G.V. Asadi, C.M. Read, A.M. Kobos, *Cathode shell stress modeling*; http://www.genisim.com/website/tms91.htm
10. A.M. Morega, V.M. Petre, A. Panaitescu, *Current flow and heat transfer in aluminum electrolysis cell – a FEM Analysis*, ATEE, 2006.
11. A. Moraru, A.M. Morega, M.V. Petre, M. Cilianu, *Magnetohydrodynamic flow simulation in an aluminum electrolysis cell*, Rev. Roum. Sci. Techn. – Électrotechn. et Énerg., **56**, *1*, pp. 131-140, 2011.
12. M.V. Petre, *Electro-thermal and flow processes in aluminum electrolysis*, PhD Thesis, Faculty of Electrical Engineering, University "Politehnica" of Bucharest, 2011.
13. C.I. Mocanu, *Bazele electrotehnicii – Teoria câmpului electromagnetic* (2nd ed.), Edit. Didactică şi Pedagogică, Bucureşti, 1991.
14. * * *, Autodesk Inventor, v. 9.0, 2009, Autodesk, San Rafael, California, USA.
15. * * *, COMSOL Multiphysics, v. 3.5a, 2010.
16. * * *, International Union of Pure and Applied Chemistry (IUPAC), *Definition of terms relating to the non-ultimate mechanical properties of polymers*, Pure & Appl. Chem, **70**, 3, pp. 701-754, 1998.
17. * * *, Smartview 1.8.0.6, 2006, *Fluke Thermography*, 3550 Annapolis Lane, Plymouth, MN 55447, USA.